Biofilm-associated Mycobacterium abscessus cells have altered antibiotic tolerance and surface glycolipids in Artificial Cystic Fibrosis Sputum Media.

Augusto Cesar Hunt[1], Joseph Boll[1] and Cara Boutte[1*]

[1]Department of Biology, University of Texas Arlington

[*]Corresponding author: cara.boutte@uta.edu

Abstract

Mycobacterium abscessus (*Mab*) is a biofilm-forming, multi-drug resistant, non-tuberculous mycobacterial (NTM) pathogen increasingly found in Cystic Fibrosis patients. Antibiotic treatment for these infections is often unsuccessful, partly due to Mab's high intrinsic antibiotic resistance. It is not clear whether antibiotic tolerance caused by biofilm formation also contributes to poor treatment outcomes. We studied the surface glycolipids and antibiotic tolerance of *Mab* biofilms grown in Artificial Cystic Fibrosis Sputum media in order to determine how they are affected by nutrient conditions that closely mimic infection. We found that *Mab* biofilms grown in ACFS display more of the virulence lipid trehalose dimycolate than biofilms grown in standard lab media. Biofilms in ACFS media also afford more protection against clinically important antibiotics than biofilms grown in lab media. These results indicate that *Mab* cell physiology in biofilms depends on environmental factors, and that nutrient conditions found within Cystic Fibrosis infections could contribute to both increased virulence and antibiotic tolerance.

Introduction

Infections caused by Non-Tuberculous Mycobacteria (NTM) are on the rise across the globe (1-3). *Mycobacterium abscessus* (*Mab*) is a highly antibiotic-resistant NTM that causes soft tissue infections and is an increasingly common respiratory pathogen in Cystic Fibrosis (CF) patients

27 (4-6). While most NTM infections are believed to be contracted through environmental
28 exposure, *Mab* has recently been shown to be transmitted between CF patients, probably by
29 fomites (7). Unfortunately, *Mab* infections in CF patients are very difficult to treat, and there are
30 no standardized treatment regimens. Treatment usually involves some combination of
31 clarithromycin, amikacin, imipenem, cefoxitin and/ or linezolid (8). Infection clearance after up to
32 3 years of antibiotic treatment is achieved in only 10-55% of patients (8). This level of treatment
33 failure is likely partly due to intrinsic antibiotic resistance (9-11); however, antibiotic tolerance
34 may also play a role (12), though the environmental conditions that may induce tolerance in this
35 organism are poorly understood.
36
37 The pathophysiology of *Mab* infection in the CF lung has scarcely been studied, but one
38 pathology study of explanted lungs from CF patients showed *Mab* aggregates that appear to be
39 forming a biofilm around the alveoli (13). Biofilms are bacterial communities that, in many
40 species are held together by exopolysaccharides (14). Mycobacterial biofilms appear to depend
41 on surface glycolipids (15) and free mycolic acids (16, 17), though many questions remain about
42 the composition of the matrix in mycobacterial biofilms. Because bacteria growing in biofilms are
43 notoriously tolerant to antibiotics (18), this mode of growth during infection may contribute to the
44 treatment recalcitrance of *Mab*. While we currently lack a comprehensive model of the chemical
45 and genetic basis of *Mab* biofilm formation, it is clear that surface glycolipids are important.
46 Glycopeptidolipids, which are found on the outer leaflet of the mycobacterial outer membrane,
47 have been shown to affect biofilm structure (19) and are thought to modulate the course of
48 infection (20, 21). Trehalose mycolates, which are known to contribute to virulence in *Mtb* (22)
49 are also found on the surface of some *Mab* strains, though their contribution to biofilm formation
50 and virulence in *Mab* has not been studied.
51

52 *Mab* has two genetic isoforms: the wild-type “smooth” strains, which produce abundant GPLs
53 and have less trehalose mycolates; and spontaneous “rough” mutants, which have genetic
54 lesions in the GPL loci, and display little or no GPLs but have higher levels of trehalose
55 mycolates (23, 24). The smooth strains form more robust biofilms and it is thought that this form
56 could contribute to colonization at infection sites (24), which is likely helped by the GPLs, which
57 mask other cell surface molecules that activate innate immunity (21). The rough mutants cause
58 more inflammation (21), are more virulent, and are thought to promote more tissue invasion
59 (24). Rough mutants are more frequently isolated after a persistent infection has been
60 established for a long period, in both CF and non-CF patients (25, 26).
61
62 The smooth and rough genetic variants represent two phenotypic extremes of *M. abscessus*
63 physiology. However, the rough variants only form in some infections, and it is thought that most
64 infections are established by smooth strains (24). Smooth strains are known to form biofilms *in*
65 *vitro* (12, 19) and are thought to also form biofilms during infection (13). Antibiotic-recalcitrant
66 *Mab* infections are likely to involve mature biofilms growing in complex nutrient environments.
67 However, the *in vitro Mab* biofilm studies have been done on immature biofilms in simple
68 nutrient environments (12, 19): in these conditions there are modest differences in antibiotic
69 tolerance between biofilm-associated and planktonic cells (19). Thus, it is not clear to what
70 extent biofilms contribute to antibiotic tolerance during infection.
71
72 In this work, we sought to determine how biofilm formation, surface glycolipids and antibiotic
73 tolerance are affected by media conditions in a *Mab* smooth strain, ATCC19977. We find that
74 the cell surface physiology of *Mab* in Artificial Cystic Fibrosis Sputum (ACFS) media is very
75 different from that observed in either minimal HdB media or in the typical mycobacterial growth
76 media, 7H9. While smooth *Mab* makes GPLs in all these media types, it displays more

77 trehalose mycolates in the ACFS media. We also observe more relative antibiotic tolerance in
78 biofilm-associated than planktonic cells in the ACFS media.

79 **Results**

80 To determine how different nutrient conditions affect basic cell physiology, we measured growth
81 rate and microscopically examined *Mab* in three different media. *Mab* grows fastest in 7H9
82 media (Fig 1AB), even though the Artificial Cystic Fibrosis Sputum (ACFS) media is richer(27).
83 We imaged cells using phase microscopy and observed that cell lengths were longer in ACFS
84 media (Fig. 1CD). We stained cells in log phase in each media with both NADA, a fluorophore-
85 conjugated D-alanine (28) that is integrated into peptidoglycan, and FM4-64, which is thought
86 to primarily stain the inner membrane. Although growth rates were more similar in HdB and
87 ACFS media, cell surface staining was more similar in HdB and 7H9. The NADA staining was
88 consistent with studies performed in other mycobacterial cells: brighter staining at the septa and
89 poles where new peptidoglycan is inserted (29). FM4-64 stained most cells in these media types
90 dimly, but a subset stained more brightly. Staining of cells in ACFS media was dim and
91 consistent (Fig. 1DE). We observed in the phase images that cells growing in ACFS appear to
92 be encased in translucent sheaths, which may impede access of the stains (Fig. 1D). These
93 data show that *Mab* is physiologically different in typical lab media than in media that mimics the
94 conditions in lungs of Cystic Fibrosis patients.

95

96 In order to study the physiology of biofilms, we sought to develop a method to separate biofilm
97 and planktonic cells from the same culture well: this allows us to control internally for nutrient
98 depletion in the media, which also impacts cell physiology and antibiotic tolerance. Tissue-
99 treated plates allowed cells to aggregate at the bottom of each well, while the planktonic cells
100 remained in the clear media in the upper half of the well. We pipetted off all the clear media on
101 the top of each well to isolate planktonic cells. We resuspended the surface-associated cells on
102 the bottom of the plate in 7H9 with tween80, a non-ionic detergent, which broke apart cell

103 clumps. To determine whether 7H9 + tween80 was sufficient to break apart clumps or whether
104 sonication was necessary, we compared the colony forming units (CFU) produced from biofilm
105 resuspensions with and without sonication (Fig. S1). Sonication did not change the CFU counts,
106 so we conclude that resuspension in 7H9 + tween80 alone is sufficient to break apart smooth
107 *Mab* biofilms. Therefore, we used that method for biofilm enumeration in subsequent
108 experiments.
109
110 We next analyzed how the three media types affect biofilm development and morphology. We
111 grew *Mab* in the three different media types over time and monitored biofilm development by
112 CFU assay and photography. Biofilms growing in all media types reach maximal cell density by
113 day 6, though cell density increases more slowly in the HdB minimal media (Fig. 2). Biofilms in
114 ACFS are three-dimensional and wrinkled, similar to the cording seen in mycobacterial colonies
115 and pellicle biofilms. We see no cording in biofilms grown in HdB or 7H9, and the surface of
116 those biofilms looks dry and flat. We never observed thick pellicles in the media conditions we
117 tested, but in 7H9 and HdB media we observed small floating islands of thin, translucent, waxy-
118 looking pellicle (Fig. 2). From these data we conclude that biofilm morphology was affected by
119 media condition.
120
121 To probe the physiological differences between biofilm and planktonic cells in our assay, we
122 tested the ability of biofilm and planktonic cells to transcriptionally and translationally respond to
123 induction of an inducible reporter. We transformed *Mab* with a plasmid that expresses Tag-RFP
124 under the control of a constitutive P_{GroEL} promoter, and expresses eGFP under control of an
125 inducible $P_{nitrile}$ promoter. We allowed biofilms of this culture to mature for 6 days, then induced
126 them with isovaleronitrile, which should induce expression of eGFP. After 24 hours of induction,
127 we resuspended and fixed cells from the planktonic and biofilm populations in each media type,
128 and visualized the cells by fluorescence microscopy (Fig. 3A). We found that in all media

129 conditions, cells in biofilm were less likely than planktonic cells to express significant eGFP
130 upon induction, compared to the constitutive Tag-RFP (Fig. 3B). This shows that biofilm cells
131 are either less permeable to the inducer, or are less transcriptionally and translationally active
132 than planktonic cells in the same culture well, or both. These data also validate our method of
133 separating planktonic cells from biofilm cells, by showing separated cell types are
134 physiologically distinct in all three media types.
135
136 We hypothesized that the difference in biofilm structure and texture might be due to differences
137 in various glycolipids produced during biofilm development in the different media types. We
138 extracted surface glycolipids from mature biofilms grown in all three media conditions and
139 separated them by thin layer chromatography (TLC). TLC analysis showed that GPLs are
140 present in all conditions, as expected for smooth *Mab* strains (Fig. 4A,C). However, we
141 observed two major lipid species found in the ACFS biofilms that were not present in either the
142 planktonic cultures nor in biofilms grown in HdB or 7H9 (Fig. 4AB,D). Based on previous GPL
143 analysis (24), the purple spot near the top (Fig. 4A, spot b) is an unidentified wax, while the
144 dark purple spot at the bottom (Fig. 4A, spot d) is trehalose dimycolate (TDM). We observe a
145 statistically significant increase in the wax species in ACFS (Fig. 4B). The levels of GPLs
146 appear to be similar on the TLC, and we don't see significant differences by quantifying the
147 spots (Fig. 4A,C). The purple TDM spot, d, looks significantly brighter in the TLC, but because it
148 overlaps with lower GPL species, we were not able to show a significant difference by
149 quantification (Fig. 4A,D). These data show that media conditions affect the surface glycolipid
150 expression of *Mab* and that biofilms in ACFS media have higher levels of wax and TDM, a
151 glycolipid that is a virulence factor in *Mtb* infections (22).
152
153

154 To best study the antibiotic tolerance of *Mab* biofilms, we worked to identify the stage of biofilm
155 development that provided the most tolerance for biofilm cells compared to planktonic cells. For
156 these and all subsequent biofilm experiments, we compared survival of biofilm and planktonic
157 cells from the same well of a 24-well plate for each replicate. We incubated *Mab* in ACFS media
158 for 3, 6 or 11 days, then treated each well with two clinical drugs, clarithromycin and imipenem.
159 We then measured survival over time and found that the tolerance of all cells increased in older
160 biofilms, likely due to nutrient depletion of the media (Fig. 5A). 6-day old biofilms had higher
161 tolerance compared to the planktonic cells in the same well at both 24 and 48 hours of
162 treatment (Fig. 5B). From this, we conclude that at 6 days the biofilms in our assays are mature
163 enough to substantially protect cells against antibiotics. Based on these results, we conducted
164 all subsequent biofilm assays with 6 day old biofilms.
165
166 In order to determine how media type affects the tolerance of *Mab* biofilms to clinically used
167 antibiotics, we treated 6-day old biofilms grown in different media types with varying
168 concentrations of the clinically used antibiotics amikacin, clarithromycin and cefoxitin, and then
169 plated both the biofilm and planktonic cells at 48 hours after treatment. We found that amikacin
170 consistently killed planktonic cells at nearly an order of magnitude more than the biofilm cells
171 from the same well, across media types. With clarithromycin and cefoxitin treatment, however,
172 we saw much more variability in antibiotic tolerance across media types. With both these
173 antibiotics, biofilm cells were only slightly more tolerant than planktonic cells in both 7H9 and
174 HdB, while biofilm cells were much more tolerant in ACFS. Clarithromycin was the only drug
175 that was able to kill biofilm cells at concentrations below 50 μg/ml, and this only occurred in
176 ACFS media (Fig. 6). These data indicate that media conditions have a substantial impact on
177 aspects of biofilm physiology that control antibiotic tolerance. More specifically, these data show
178 that the biofilm itself yields more protection against clarithromycin and cefoxitin in ACFS media,
179 while tolerance is due to non-biofilm causes in 7H9 and HdB media.

180

181 **Discussion**

182 Bacterial physiology is enormously plastic. Bacterial cell size, shape, growth rates, surface
183 properties and gene expression all change profoundly even between different lab media
184 conditions (30-32). This plasticity makes it very difficult to determine the physiological state of a
185 pathogen during infection. In this study, we sought to physiologically profile the emerging
186 pathogen *M. abscessus* in two standard lab growth medias and one media designed to mimic
187 the nutrient conditions in the lungs of Cystic Fibrosis patients (ACFS). We find that, compared to
188 standard lab medias, ACFS media induces profound physiological changes in *Mab*, both in
189 planktonic (Fig.1) and biofilm states (Fig.4, Fig.6).

190

191 Bacterial biofilms are complex structures which, on the macro scale, vary physiologically
192 according to developmental stage (33), surface type (34) and nutrient conditions (35). On the
193 microscopic scale, there is also heterogeneity within a single biofilm: cells in different places
194 within the biofilm express different surface factors and have different gene expression profiles
195 (36-38). Thus, it is not meaningful to merely compare the phenotypes of “biofilm” and
196 “planktonic” cells from a given species, as there is enormous phenotypic variety within each of
197 these categories. In this work, we profiled some of the phenotypic diversity possible in *Mab*
198 biofilms in order to assess the extent to which *in vitro* biofilm experiments might be relevant to
199 the physiology of *Mab* biofilms within the lungs of CF patients. Our results show that *Mab*
200 biofilms in ACFS media have important physiological differences from biofilms in the standard
201 mycobacterial lab medias HdB and 7H9 (Fig. 2, Fig.4, Fig.6). The fact that such differences can
202 be seen even between *in vitro* media conditions shows that *Mab* biofilm physiology is
203 responsive to environmental conditions. We hypothesize that *Mab* physiology in HdB and 7H9
204 media is unlikely to represent its physiology during infection.

205

206 While all experiments herein were performed with the smooth *Mab*, which produces
207 glycopeptidolipids (GPLs), we observed differences in the appearance of the biofilms that
208 formed in the different media types. The biofilms in both HdB and 7H9 appeared dry, flat and
209 flaky, while the biofilms that formed in the ACFS media looked wet and appeared to form cords
210 at early stages and tendrils later on (Fig. 2). These differences could be merely due to the
211 chemical and viscosity differences between the media types, or they could be due to changes in
212 *Mab* cell physiology in the different media types. We profiled the surface glycolipids and
213 antibiotic sensitivity of cells in these different biofilms, and found that cells in ACFS biofilms are
214 physiologically distinct: they display more trehalose dimycolate and a non-polar wax species
215 than biofilms in 7H9 and HdB (Fig. 4) and they exhibit more relative antibiotic tolerance
216 compared to planktonic cells (Fig. 6).
217
218 Because nutrient availability affects the physiology of cells within a biofilm, we sought to develop
219 methods that would allow us to disentangle responses to nutrients from responses to biofilm
220 formation. Other groups solved this problem by moving biofilms to fresh media each day (12,
221 19). We assumed that nutrients would not be unlimited during infection, and so worked to
222 assess biofilm physiology in nutrient-limited culture. First, we profiled the development of *Mab*
223 biofilms in the three media types to identify the time at which nutrients became limiting in each
224 media type. The number of cells in the biofilm peaked by 6 days of static incubation in closed
225 culture wells in all three media types (Fig. 2), so we did subsequent assays on 6-day old
226 biofilms. In order to control for the well-known effects of nutrient limitation on antibiotic tolerance
227 (39), we compared biofilm and planktonic cells from the same culture wells. These cells are
228 sharing the same depleted nutrients, so differences in physiology should be due to association
229 with the biofilm. We found that association with biofilms is protective against amikacin treatment
230 in all media types, but that sensitivity to clarithromycin and cefoxitin was variable (Fig.6). While
231 we observed considerable antibiotic tolerance in 7H9 and HdB against clarithromycin and

232 cefoxitin, the degree of tolerance does not differ very much between the planktonic and biofilm
233 associated cells (Fig. 6B,C). This implies that antibiotic tolerance in these media conditions is
234 due to some other environmental factor, such as nutrient depletion, rather than due to the
235 protection of the biofilm itself.
236
237 A previous study examined the antibiotic tolerance of smooth *Mab* biofilms in nutrient-replete
238 7H9 and found only three to four-fold increases in tolerance due to biofilm association (19). Our
239 results imply that this modest degree of antibiotic tolerance afforded by biofilm association may
240 be a function of the culture conditions. Our data show that mature biofilms grown in ACFS
241 media afford considerable protection against three clinical antibiotics from different classes.
242 These results imply that the formation of biofilms during infection in CF patients may contribute
243 to antibiotic tolerance and the difficulty of clearing *Mab* infections. Thus, treatments that could
244 help disrupt *Mab* biofilms or prevent their establishment could help clear these infections more
245 quickly. A deeper understanding of the chemistry and genetics of biofilm formation in *M.*
246 *abscessus* will be needed in order to determine the role of biofilms in infection and treatment
247 recalcitrance and to develop better treatment protocols.
248 **Materials and Methods**
249 *Media and culture conditions.* All *M. abscessus* ATCC19977 cultures were started in 7H9
250 (Becton-Dickinson, Frankin Lakes, NJ) media with 5 g/l bovine serum albumin, 2g/l dextrose,
251 0.85 g/l NaCl, 0.003 g/l catalase, 0.2% glycerol and 0.05% Tween80 and shaken overnight at
252 37C until in log phase. All *Mab* CFUs were performed by plating serial dilutions on LB Lennox
253 agar. Three media types varying in nutrient richness were used for all biofilm assays: tween80
254 was not added to any media for biofilm assay. Hartmans de Bont (HdB) Minimal Media was
255 made as described (40) 7H9 for biofilms was made as above, without the tween80. Artificial
256 Cystic Fibrosis Sputum (ACFS) media was made as described (41), except amino acids were

257 added separately, amino acids stocks for ACFS media were prepared as previously described
258 (27).
259
260 *Biofilm assays.* Log-phase *Mab* cultures in 7H9 were inoculated into tissue-culture treated 24-
261 well plates with 2mL of the appropriate media to a final optical density of 0.02. Prior to
262 incubation, each plate was covered with a Breathe-Easy sealing membrane (Electron
263 Microscope Sciences)to avoid allow air exchange but reduce evaporation. Standing biofilm
264 plates were incubated at 37C. The Breathe-Easy membrane was removed after biofilm
265 development in order to add antibiotics at the indicated time points and concentrations. The
266 biofilm plates were then re-sealed and incubated again at 37C for 24 or 48 hours. For each data
267 point, cells from three independent wells were used to calculate CFUs. Media was extracted
268 from each well without disturbing the biofilm, and plated for CFUs in assays which examined
269 planktonic cells. The remaining biofilm was re-suspended in 7H9 + tween80 and serial dilutions
270 were plated and incubated at 37°C for 4 days. Serial dilutions were done in 96-well plates in
271 7H9 + tween80 and plated on plain LB Agar plates.
272
273 *Glycolipid extractions and Thin layer chromatography.* Mature biofilms were grown in all 3
274 medias as previously mentioned. GPLs were extracted as described (31) and spotted on TLC
275 Silica Gel 60 plates (Millipore Sigma). In short, biofilms were isolated and centrifuged. Pellets
276 were resuspended for lipid extraction in 10mL Choloform/Methanol (2:1). Extractions were done
277 twice at room temperature for 24 hours and then centrifuged at 5000rpm for 30 minutes to
278 collect organic supernatant. Organic samples (Lipids) were evaporated with nitrogen and
279 resuspended in 1mL Chloroform/methanol (2:1) and treated with equal volume 0.2M NaOH (in
280 methanol). Lipids were incubated at 37C for 30 minutes and then neutralized with a few drops of
281 glacial acetic acid. Solvents were evaporated and the lipids were resuspended with
282 Choloroform/Methanol/Water (4:2:1). Samples were then centrifuged at 5000 rpm for 10

283 minutes to collect the organic layer. The solvent was evaporated and the remaining lipids were
284 resuspended in 100uL of Chloroform/methanol (2:1) and spotted. TLCs were developed in
285 Chloroform/Methanol/Water (100:14:0.8) as described (24). Plates were visualized with 10%
286 Sulfuric Acid (in ethanol) and baked for 20 minutes at 120C. The intensity of spots and the
287 intensity of all the spots in a lane (all in triplicates) were analyzed and quantified using ImageJ
288 software.
289
290 *Microscopy.* Mab cells were resuspended as above, then fixed with 4% paraformaldehyde in
291 PBS at room temperature for 2 hours. Cells were immobilized on agarose pads and imaged
292 using a Nikon Ti-2 widefield epifluorescence microscope with a Photometrics Prime 95B camera
293 and a Plan Apo 100X, 1.45 NA objective. Green fluorescent images were taken using a 96362
294 filter cube and red fluorescent images were taken using a 96365 filter cube. Images were
295 captured using NIS Elements software and analyzed using FIJI and MicrobeJ (42).
296
297 **References**
298
299 1. **World Health Organization**. 2016. Global Tuberculosis Report.

300 2. **Brode SK**, **Daley CL**, **Marras TK**. 2014. The epidemiologic relationship between
301 tuberculosis and non-tuberculous mycobacterial disease: a systematic review. int j
302 tuberc lung dis **18**:1370–1377.

303 3. **Stout JE**, **Koh W-J**, **Yew WW**. 2016. Update on pulmonary disease due to non-
304 tuberculous mycobacteria. International Journal of Infectious Diseases **45**:123–134.

305 4. **Cystic Fibrosis Foundation**. 2017. 2016 Patient Registry Annual Data Report 1–
306 94.

307 5. **Bar-On O**, **Mussaffi H**, **Mei-Zahav M**, **Prais D**, **Steuer G**, **Stafler P**, **Hananya S**,
308 **Blau H**. 2015. Increasing nontuberculous mycobacteria infection in cystic fibrosis.
309 Journal of Cystic Fibrosis **14**:53–62.

310 6. **Esther CR Jr**, **Esserman DA**, **Gilligan P**, **Kerr A**, **Noone PG**. 2010. Chronic
311 Mycobacterium abscessus infection and lung function decline in cystic fibrosis.
312 Journal of Cystic Fibrosis **9**:117–123.

313 7. **Bryant JM**, **Grogono DM**, **Rodriguez-Rincon D**, **Everall I**, **Brown KP**, **Moreno P**,
314 **Verma D**, **Hill E**, **Drijkoningen J**, **Gilligan P**, **Esther CR**, **Noone PG**, **Giddings O**,
315 **Bell SC**, **Thomson R**, **Wainwright CE**, **Coulter C**, **Pandey S**, **Wood ME**,
316 **Stockwell RE**, **Ramsay KA**, **Sherrard LJ**, **Kidd TJ**, **Jabbour N**, **Johnson GR**,
317 **Knibbs LD**, **Morawska L**, **Sly PD**, **Jones A**, **Bilton D**, **Laurenson I**, **Ruddy M**,
318 **Bourke S**, **Bowler ICJW**, **Chapman SJ**, **Clayton A**, **Cullen M**, **Dempsey O**,
319 **Denton M**, **Desai M**, **Drew RJ**, **Edenborough F**, **Evans J**, **Folb J**, **Daniels T**,
320 **Humphrey H**, **Isalska B**, **Jensen-Fangel S**, **Jönsson B**, **Jones AM**, **Katzenstein**
321 **TL**, **Lillebaek T**, **MacGregor G**, **Mayell S**, **Millar M**, **Modha D**, **Nash EF**, **O'Brien**
322 **C**, **O'Brien D**, **Ohri C**, **Pao CS**, **Peckham D**, **Perrin F**, **Perry A**, **Pressler T**, **Prtak**
323 **L**, **Qvist T**, **Robb A**, **Rodgers H**, **Schaffer K**, **Shafi N**, **van Ingen J**, **Walshaw M**,
324 **Watson D**, **West N**, **Whitehouse J**, **Haworth CS**, **Harris SR**, **Ordway D**, **Parkhill**
325 **J**, **Floto RA**. 2016. Emergence and spread of a human-transmissible multidrug-
326 resistant nontuberculous mycobacterium. Science **354**:751–757.

327 8. **DaCosta A**, **Jordan CL**, **Giddings O**, **Lin F-C**, **Gilligan P**, **Esther CR Jr**. 2017.
328 Outcomes associated with antibiotic regimens for treatment of Mycobacterium
329 abscessus in cystic fibrosis patients. Journal of Cystic Fibrosis 1–5.

330 9. **Rominski A**, **Selchow P**, **Becker K**, **Brülle JK**, **Dal Molin M**, **Sander P**. 2017.

331 Elucidation of Mycobacterium abscessus aminoglycoside and capreomycin
332 resistance by targeted deletion of three putative resistance genes. Journal of
333 Antimicrobial Chemotherapy 1–10.

334 10. **Rominski A**, **Roditscheff A**, **Selchow P**, **Böttger EC**, **Sander P**. 2017. Intrinsic
335 rifamycin resistance of Mycobacterium abscessusis mediated by ADP-
336 ribosyltransferase MAB_0591. Journal of Antimicrobial Chemotherapy **72**:376–384.

337 11. **Hurst-Hess K**, **Rudra P**, **Ghosh P**. 2017. Mycobacterium abscessus WhiB7
338 Regulates a Species-Specific Repertoire of Genes To Confer Extreme Antibiotic
339 Resistance. Antimicrobial Agents and Chemotherapy **61**:e01347–17–11.

340 12. **Greendyke R**, **Byrd TF**. 2008. Differential Antibiotic Susceptibility of
341 Mycobacterium abscessus Variants in Biofilms and Macrophages Compared to
342 That of Planktonic Bacteria. Antimicrobial Agents and Chemotherapy **52**:2019–
343 2026.

344 13. **Qvist T**, **Eickhardt S**, **Kragh K**, **Andersen C**, **Iverson M**, **Høiby N**, **Bjarnsholt T**.
345 2015. Chronic pulmonary disease with Mycobacterium abscessus complex is a
346 biofilm infection. Eur Respiratory Soc. **46**:1823–1826.

347 14. **Flemming HC**, **Neu TR**, **Wozniak DJ**. 2007. The EPS Matrix: The “House of
348 Biofilm Cells.” J Bacteriol **189**:7945–7947.

349 15. **Recht J**, **Martínez A**, **Torello S**, **Kolter R**. 2000. Genetic analysis of sliding motility
350 in Mycobacterium smegmatis. J Bacteriol **182**:4348–4351.

351 16. **Ojha A**, **Anand M**, **Bhatt A**, **Kremer L**, **Jacobs WR Jr.**, **Hatfull GF**. 2005. GroEL1:
352 A Dedicated Chaperone Involved in Mycolic Acid Biosynthesis during Biofilm

353 Formation in Mycobacteria. Cell **123**:861–873.

354 17. **Ojha AK**, **Baughn AD**, **Sambandan D**, **Hsu T**, **Trivelli X**, **Guérardel Y**, **Alahari A**,
355 **Kremer L**, **Jacobs WR Jr.**, **Hatfull GF**. 2008. Growth of Mycobacterium
356 tuberculosisbiofilms containing free mycolic acids and harbouring drug-tolerant
357 bacteria. Mol Microbiol **69**:164–174.

358 18. **Stewart P**. 2015. Antimicrobial tolerance in biofilms. Microbiology Spectrum
359 **doi:10.1128/microbiolspec.MB-0010-2014**.

360 19. **Clary G**, **Sasindran SJ**, **Nesbitt N**, **Mason L**, **Cole S**, **Azad A**, **McCoy K**,
361 **Schlesinger LS**, **Hall-Stoodley L**. 2018. Mycobacterium abscessusSmooth and
362 Rough Morphotypes Form Antimicrobial-Tolerant Biofilm Phenotypes but Are Killed
363 by Acetic Acid. Antimicrobial Agents and Chemotherapy **62**:e01782–17–17.

364 20. **Gutiérrez AV**, **Viljoen A**, **Ghigo E**, **Herrmann J-L**, **Kremer L**. 2018.
365 Glycopeptidolipids, a Double-Edged Sword of the Mycobacterium abscessus
366 Complex. Front Microbiol **9**:E943–8.

367 21. **Davidson LB**, **Nessar R**, **Kempaiah P**, **Perkins DJ**, **Byrd TF**. 2011.
368 Mycobacterium abscessus Glycopeptidolipid Prevents Respiratory Epithelial TLR2
369 Signaling as Measured by HβD2 Gene Expression and IL-8 Release. PLoS ONE
370 **6**:e29148–8.

371 22. **Hunter RL**, **Olsen MR**, **Jagannath C**, **Actor JK**. 2006. Multiple roles of cord factor
372 in the pathogenesis of primary, secondary, and cavitary tuberculosis, including a
373 revised description of the pathology of secondary disease. Ann Clin Lab Sci
374 **36**:371–386.

375 23. **Byrd TF**, **Lyons CR**. 1999. Preliminary characterization of a Mycobacterium
376 abscessus mutant in human and murine models of infection. Infection and immunity
377 **67**:4700–4707.

378 24. **Howard ST**. 2006. Spontaneous reversion of Mycobacterium abscessus from a
379 smooth to a rough morphotype is associated with reduced expression of
380 glycopeptidolipid and reacquisition of an invasive phenotype. Microbiology
381 (Reading, Engl) **152**:1581–1590.

382 25. **Kreutzfeldt KM**, **McAdam PR**, **Claxton P**, **Holmes A**, **Seagar AL**, **Laurenson IF**,
383 **Fitzgerald JR**. 2013. Molecular Longitudinal Tracking of Mycobacterium abscessus
384 spp. during Chronic Infection of the Human Lung. PLoS ONE **8**:e63237–9.

385 26. **Park IK**, **Hsu AP**, **Tettelin H**, **Shallom SJ**, **Drake SK**, **Ding L**, **Wu U-I**, **Adamo N**,
386 **Prevots DR**, **Olivier KN**, **Holland SM**, **Sampaio EP**, **Zelazny AM**. 2015. Clonal
387 Diversification and Changes in Lipid Traits and Colony Morphology in
388 Mycobacterium abscessus Clinical Isolates. J Clin Microbiol, 6 ed. **53**:3438–3447.

389 27. **Palmer KL**, **Aye LM**, **Whiteley M**. 2007. Nutritional Cues Control Pseudomonas
390 aeruginosa Multicellular Behavior in Cystic Fibrosis Sputum. J Bacteriol **189**:8079–
391 8087.

392 28. **Kuru E**, **Hughes HV**, **Brown PJ**, **Hall E**, **Tekkam S**, **Cava F**, **de Pedro MA**, **Brun**
393 **YV**, **VanNieuwenhze MS**. 2012. In Situ Probing of Newly Synthesized
394 Peptidoglycan in Live Bacteria with Fluorescent D-Amino Acids. Angew Chem Int
395 Ed **51**:12519–12523.

396 29. **Aldridge BB**, **Fernandez-Suarez M**, **Heller D**, **Ambravaneswaran V**, **Irimia D**,
397 **Toner M**, **Fortune SM**. 2012. Asymmetry and Aging of Mycobacterial Cells Lead to

398 Variable Growth and Antibiotic Susceptibility. Science **335**:100–104.

399 30. **Schaechter M**, **Microbiology OM**, **1958**. 1958. Dependency on Medium and
400 Temperature of Cell Size and Chemical Composition during Balanced Growth of
401 Salmonella typhimurium. J Gen Microbiol **19**:592–606.

402 31. **Ojha AK**, **Varma S**, **Chatterji D**, **(null)**. 2002. Synthesis of an unusual polar
403 glycopeptidolipid in glucose-limited culture of Mycobacterium smegmatis.
404 Microbiology **148**:3039–3048.

405 32. **Blair JMA**, **Richmond GE**, **Bailey AM**, **Ivens A**, **Piddock LJV**. 2013. Choice of
406 Bacterial Growth Medium Alters the Transcriptome and Phenotype of Salmonella
407 enterica Serovar Typhimurium. PLoS ONE **8**:e63912–8.

408 33. **Kostakioti M**, **Hadjifrangiskou M**, **Hultgren SJ**. 2013. Bacterial Biofilms:
409 Development, Dispersal, and Therapeutic Strategies in the Dawn of the
410 Postantibiotic Era. Cold Spring Harb Perspect Med **3**:a010306–a010306.

411 34. **Landry RM**, **An D**, **Hupp JT**, **Singh PK**, **Parsek MR**. 2006. Mucin-Pseudomonas
412 aeruginosa interactions promote biofilm formation and antibiotic resistance. Mol
413 Microbiol **59**:142–151.

414 35. **Jackson LMD**, **Kroukamp O**, **Wolfaardt GM**. 2015. Effect of carbon on whole-
415 biofilm metabolic response to high doses of streptomycin. Front Microbiol **6**:1114–
416 14.

417 36. **Serra DO**, **Richter AM**, **Klauck G**, **Mika F**, **Hengge R**. 2013. Microanatomy at
418 Cellular Resolution and Spatial Order of Physiological Differentiation in a Bacterial
419 Biofilm. mBio **4**:e00103–13–e00103–13.

420 37. **Besharova O**, **Suchanek VM**, **Hartmann R**, **Drescher K**, **Sourjik V**. 2016.
421 Diversification of Gene Expression during Formation of Static Submerged Biofilms
422 by Escherichia coli. Front Microbiol **7**:717–17.

423 38. **Williamson KS**, **Richards LA**, **Perez-Osorio AC**, **Pitts B**, **McInnerney K**, **Stewart**
424 **PS**, **Franklin MJ**. 2012. Heterogeneity in Pseudomonas aeruginosa Biofilms
425 Includes Expression of Ribosome Hibernation Factors in the Antibiotic-Tolerant
426 Subpopulation and Hypoxia-Induced Stress Response in the Metabolically Active
427 Population. J Bacteriol **194**:2062–2073.

428 39. **Xie Z**, **Siddiqi N**, **Rubin EJ**. 2005. Differential Antibiotic Susceptibilities of Starved
429 Mycobacterium tuberculosis Isolates. Antimicrobial Agents and Chemotherapy
430 **49**:4778–4780.

431 40. **Hartmans S**, **De Bont JAM**. 1992. The genus *Mycobacterium*— nonmedical , 2nd
432 ed. Springer-Verlag New York Inc., New York, NY.

433 41. **Sriramulu DD**. 2005. Microcolony formation: a novel biofilm model of
434 Pseudomonas aeruginosa for the cystic fibrosis lung. Journal of Medical
435 Microbiology **54**:667–676.

436 42. **Ducret A**, **Quardokus EM**, **Brun YV**. 2016. MicrobeJ, a tool for high throughput
437 bacterial cell detection and quantitative analysis. Nature Microbiology **1**:1–7

438

439

440

441 **Figures and Figure Legends**

442

443

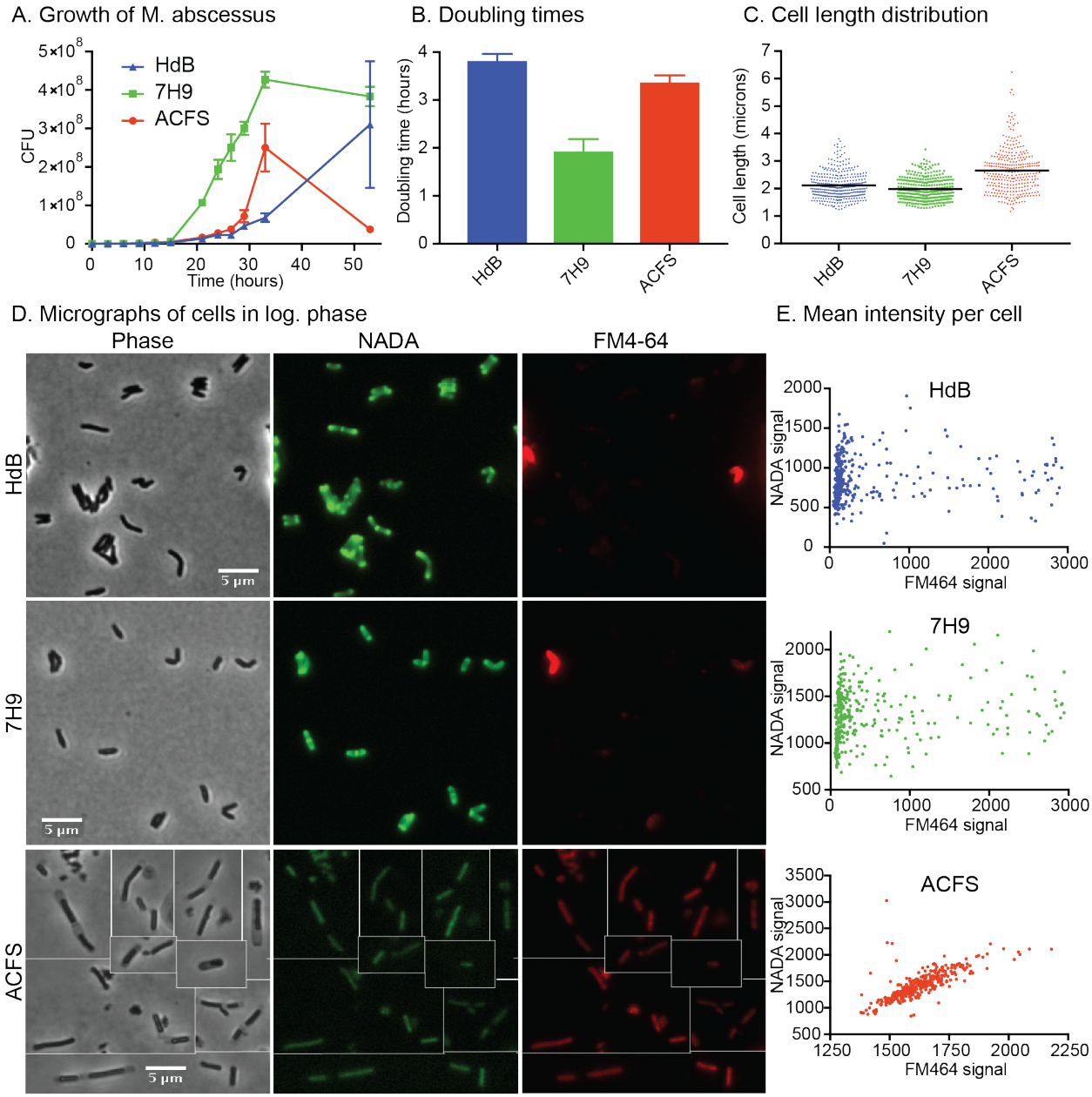

444

445 **Figure 1. The physiology of *Mab* planktonic cells varies according to media type.** A)
446 Colony forming units over time in the three growth media. B) Maximum doubling times during
447 log. phase growth, calculated from data in (A). C) Quantification of cell lengths of *Mab* cells in
448 log. phase, in the three media types. At least 300 cells from two biological replicates were
449 imaged by phase microscopy and cell lengths were calculated using MicrobeJ. D) Micrographs
450 of log phase cells stained with the fluorescent D-amino acid NADA and the membrane stain
451 FM4-64. E) Quantification of the average fluorescent intensity for at least 300 cells from two
452 biological replicates, stained with NADA and FM4-64, as in (D).

453

454

455

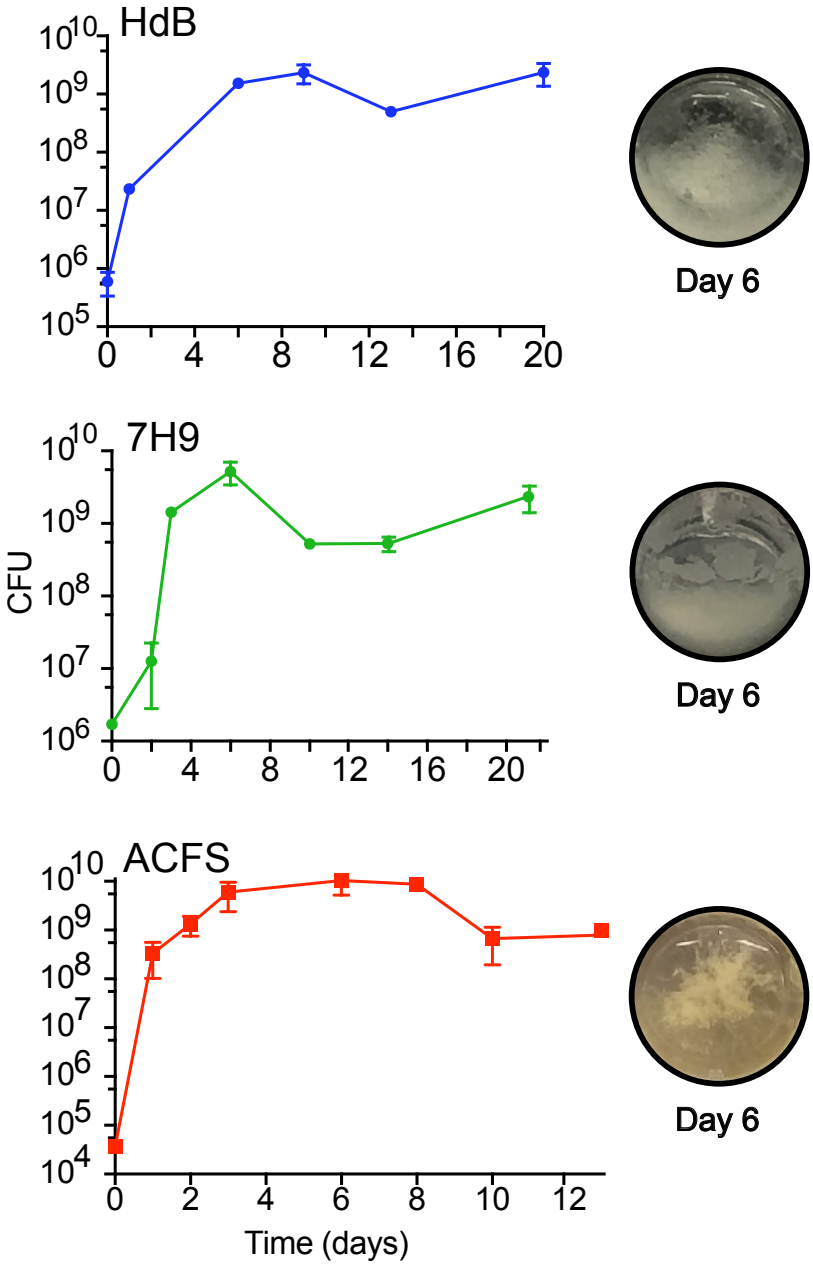

Figure 2. The development and macroscopic structure of *Mab* biofilms in different media. Colony forming units for biofilm-associated cells in standing culture over time. Images of corresponding biofilms taken at 6 days.

A. Micrographs of Live/Dead reporter in ACFS

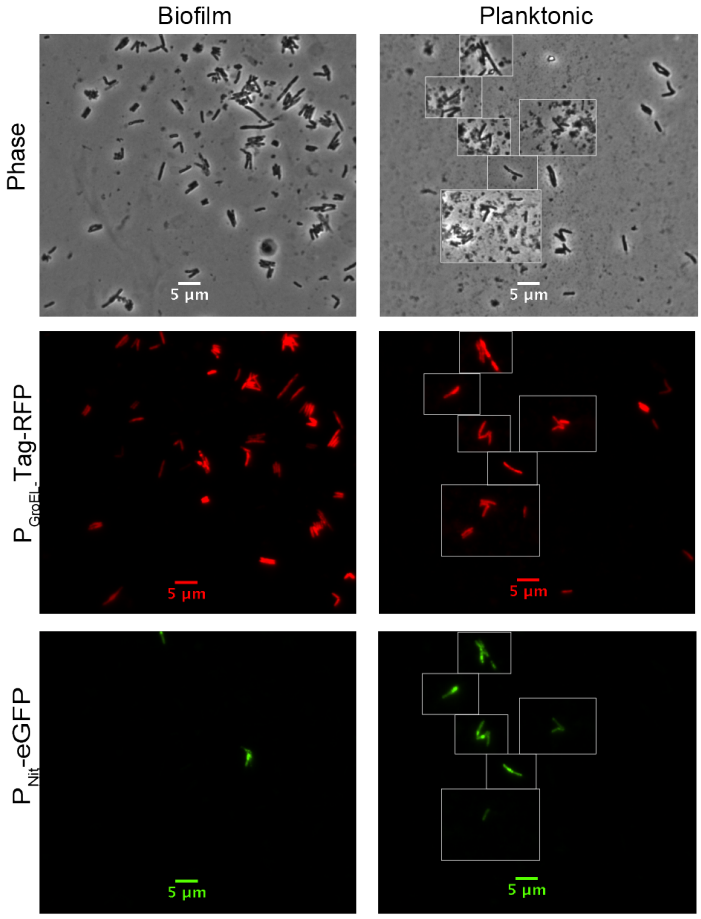

B. Percent induced in ACFS, 7H9 and HdB

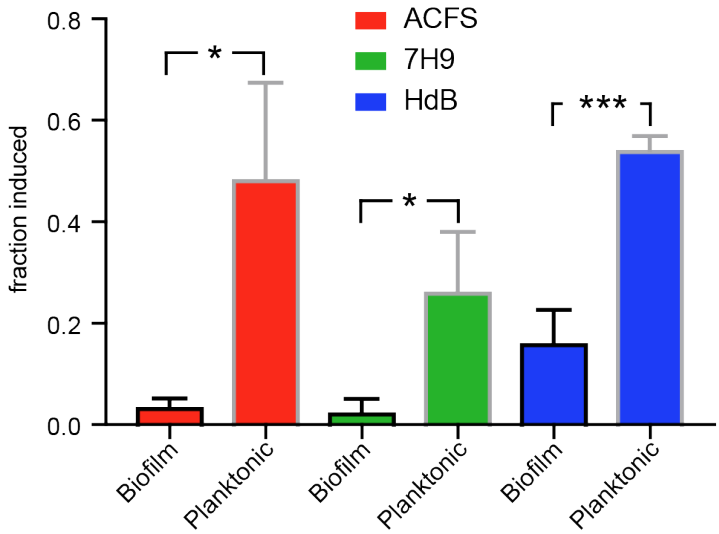

Figure 3. Cells in *Mab* biofilms are less responsive to a transcriptional inducer. (A) Micrographs of *Mab* cells carrying the pDE43-MEK-Nit-live/dead vector from biofilms grown for 6 days in ACFS, then induced with 10^{-6} isovaleronitrile for one day before fixation and imaging.

Living cells that retain the vector show constitutive Tag-RFP signal, inducible cells also show eGFP signal. (B) Percentage of cells with average red signal intensities above 400 that also have average green signal intensities above 100 in each condition. At least 100 cells each from three independent biological replicates were quantified for each condition. P-value of biofilm vs. planktonic for ACFS, 7H9 and HdB medias are 0.0152, 0.0271 and 0.0007 respectively. P-values were calculated using an unpaired t-test statistical analysis. (* P≤ 0.05, ** P ≤ 0.01, n.s. P > 0.05.)

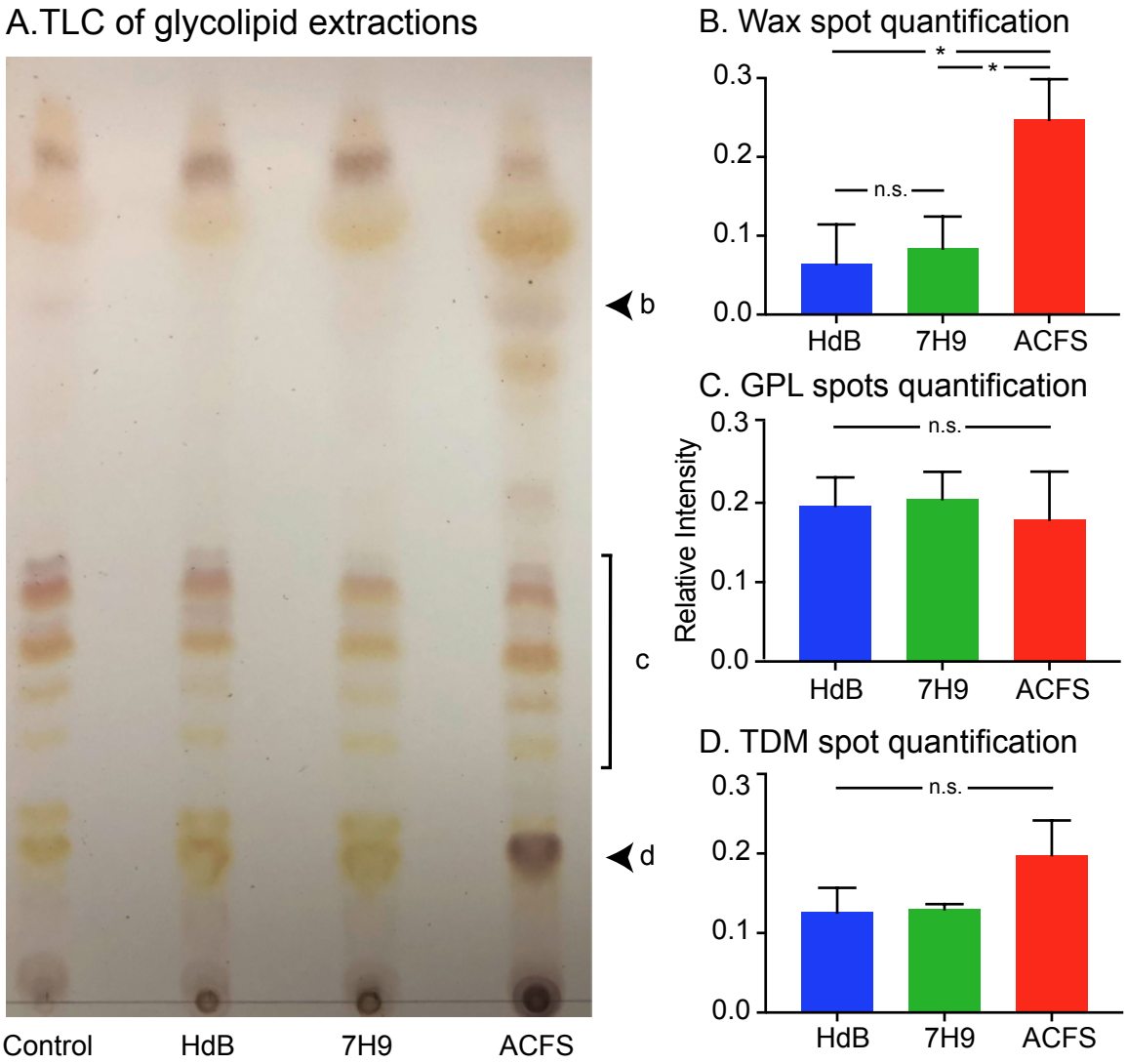

Figure 4. Lipid profiles of mature biofilms. (A) Thin Layer Chromatography (TLC) of glycolipid extracts from mature biofilms in Hdb, 7H9 and ACFS. Extraction from planktonic cells grown in 7H9 + Tween80 was used as a control sample. Black arrows indicate lipid species prominent in ACFS: b, a wax, and d, trehalose dimycolate (TDM). (B, C, D) Quantification of spot intensity over lane intensity for each media. P-values for spot b between ACFS vs. Hdb and ACFS vs. 7H9 were 0.0115 and 0.0123 respectively. P-values were calculated using a multiple t-test statistical analysis. (* P≤ 0.05, ** P ≤ 0.01, n.s. P > 0.05.)

A.Biofilm maturity affects antibiotic tolerance

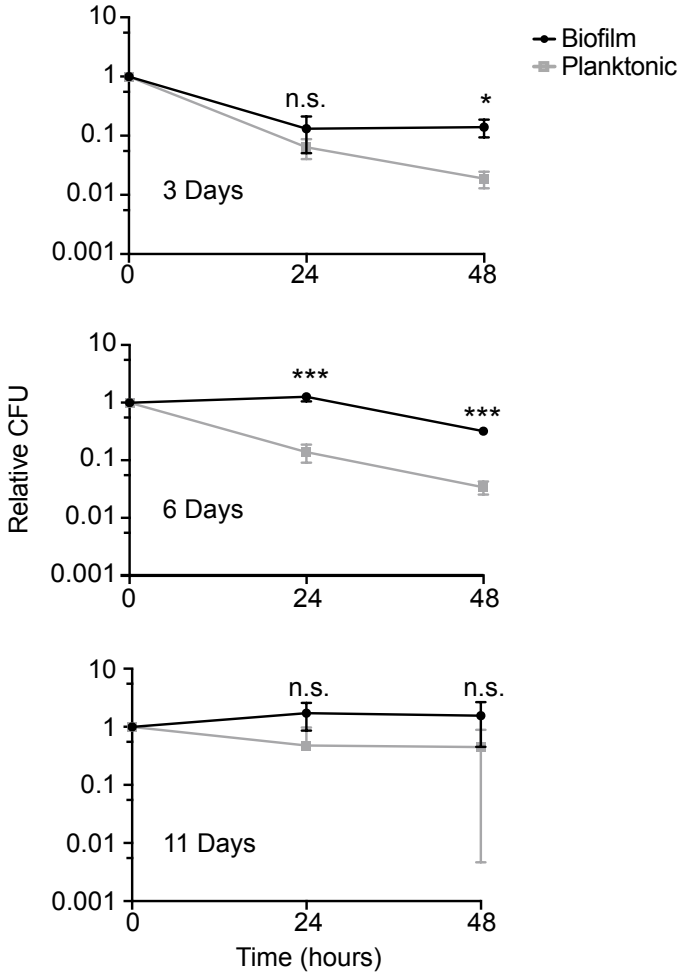

B.Percent killing at 48 hours in ACFS

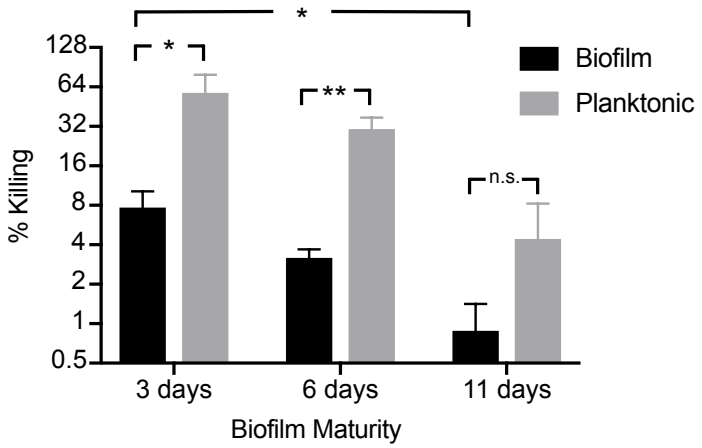

Figure 5. Antibiotic tolerance increases as ACFS biofilms mature. (A) Relative CFUs from biofilms, and planktonic cells from same well, grown for 3, 6 and 11 days in ACFS. Cultures

were treated with clarithromycin (20ug/mL) and imipenem (15ug/mL) for 48 hours, and CFUs were measured at 0, 24 and 48 hours. (B) Percent killing from 48-hour CFU time points (triplicate wells). P-values between biofilm and planktonic cells are (); for 3, 6, and 11 days respectively. P-value for biofilms between 3 and 11 days is 0.011. P-values were measured by multiple t-test statistical analysis. (* P≤ 0.05, ** P ≤ 0.01, n.s. P > 0.05.)

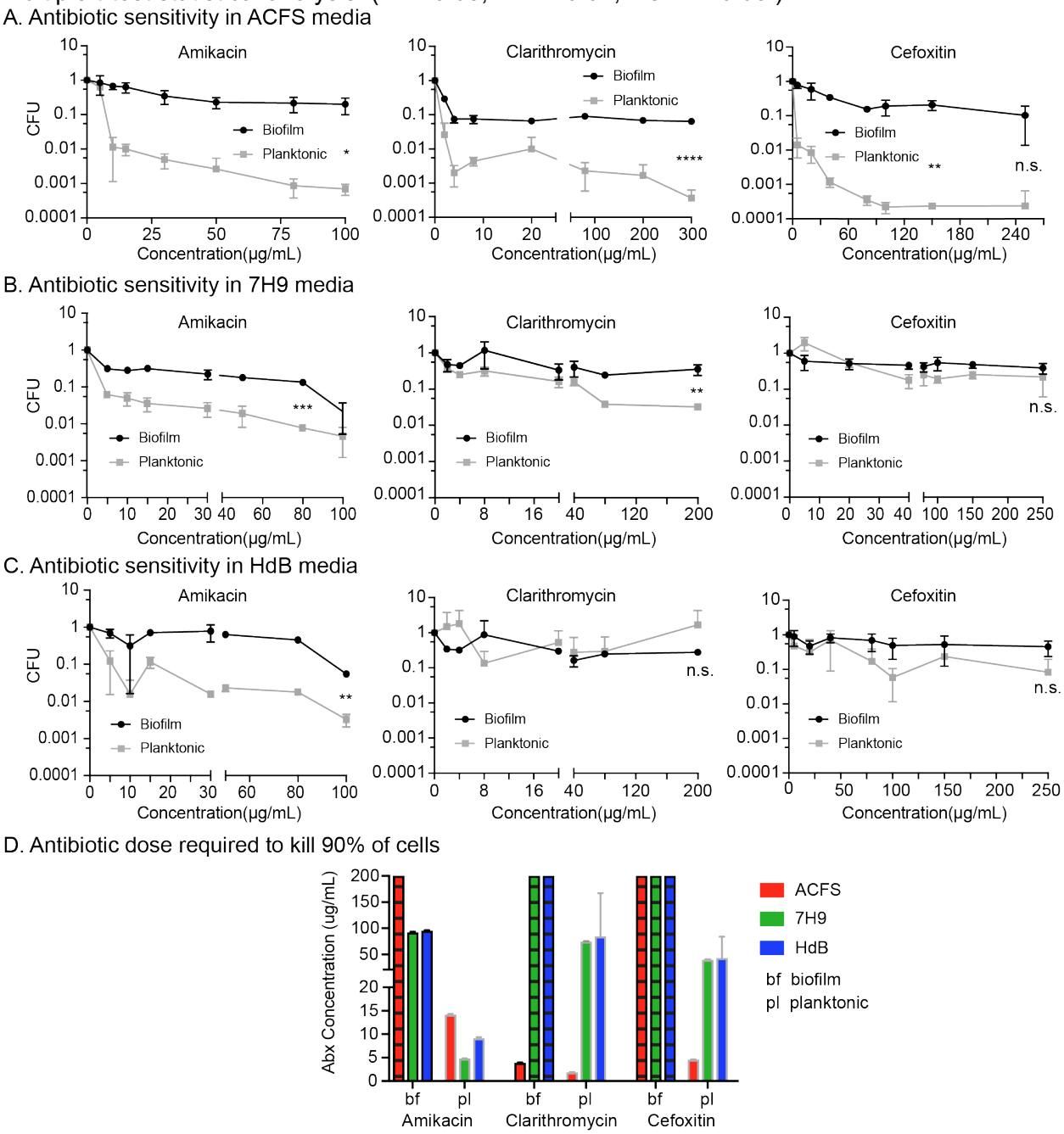

Figure 6. Antibiotic sensitivity across 3 medias. (A, B, C) CFUs of mature biofilms and planktonic cells after 48 hours of treatment with a range of antibiotic concentrations in 3 medias. Asterisks represent significance as measured by a multiple t-test statistical analysis; * P ≤ 0.05, ** P ≤ 0.01, n.s. P > 0.05. (D) LD90 graph (lethal dose for 90% killing) compares antibiotic susceptibility between medias for both biofilm and planktonic cells. Bars with hatched lines

499 indicate that we were unable to observe killing of 90% of the population at any concentration
500 used, so the LD90 is above 200 µg/mL.
501
502

503 **Supplemental Figure**

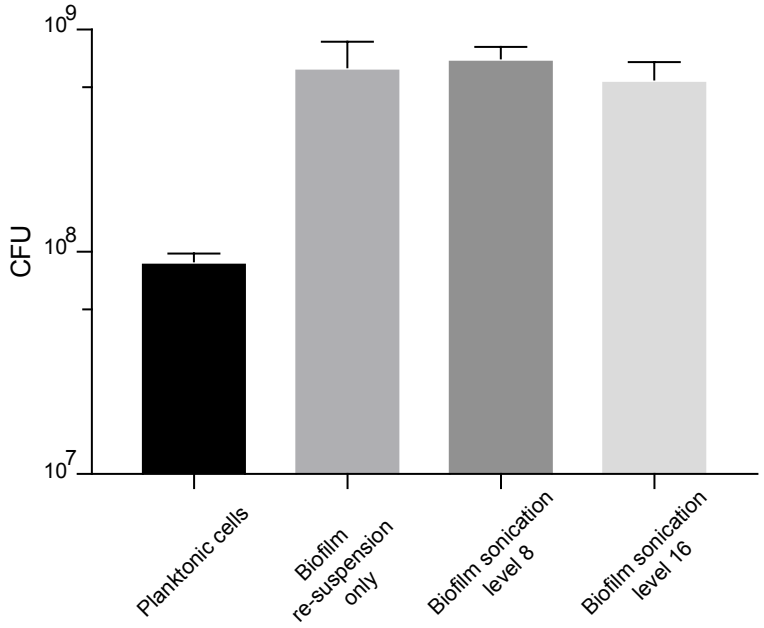

504

505 **Supplemental Figure 1. Mab Biofilm Sonication.** CFUs of mature biofilms after
506 re-suspension and sonication. Planktonic cells were used as a control. Levels of
507 sonication represent numbers on the amplitude control knob of a Microson Ultra
508 Sonic Cell Disruptor XL.